Thin Solid Films 518 (2010) 5881–5888

Contents lists available at ScienceDirect

Thin Solid Films

journal homepage: www.elsevier.com/locate/tsf

Electrochemical behaviour of self-assembly multilayer films based on iron-substituted α-Keggin polyoxotungstates

Diana M. Fernandes [a], Helena M. Carapuça [a], Christopher M.A. Brett [b], Ana M.V. Cavaleiro [a,*]

[a] Department of Chemistry/CICECO, University of Aveiro, 3810-193 Aveiro, Portugal
[b] Department of Chemistry, Faculty of Science and Technology, University of Coimbra, 3004-535 Coimbra, Portugal

ARTICLE INFO

Article history:
Received 4 November 2009
Received in revised form 25 March 2010
Accepted 7 May 2010
Available online 2 June 2010

Keywords:
Keggin
Polyoxometalates
Modified electrodes
Layer-by-layer (LBL)
Electrochemistry

ABSTRACT

Ultrathin multilayer films containing metal-substituted polyoxometalates, $[PW_{11}Fe^{III}(H_2O)O_{39}]^{4-}$ ($PW_{11}Fe$) or $[SiW_{11}Fe^{III}(H_2O)O_{39}]^{5-}$ ($SiW_{11}Fe$), and poly(ethylenimine) (PEI) were prepared by the electrostatic layer-by-layer self-assembly method on a glassy carbon electrode. The multilayer films were characterized by cyclic voltammetry and scanning electron microscopy and UV–Vis absorption spectroscopy on a quartz slide was used to monitor film growth. Cyclic voltammetry indicates that the electrochemical properties of the polyoxometalates are completely maintained in the multilayer films, and the influence of scan rate on the voltammetric features showed that the first tungsten reduction process for immobilized $PW_{11}Fe$ and $SiW_{11}Fe$ is a surface-confined process. Studies with $[Fe(CN_6)]^{3-/4-}$ as electrochemical probe showed that their permeability depends on the thickness of the multilayer films, if the outermost layer is negatively charged. Additionally, the $(PEI/SiW_{11}Fe)_n$ multilayer films showed electrocatalytic properties towards nitrite reduction.

1. Introduction

Polyoxometalates (POMs) represent a well-known class of metal–oxygen clusters with a vast variation in structure, size, composition, and properties. An important group of heteropolyanions comprises the α-Keggin polyoxometalates, with the general formula $[XM_{12}O_{40}]^{m-}$, where M is called the addenda atom, usually W or Mo. The heteroatom X may be Si or P, amongst others. Mono-lacunary species (general formula $[XM_{11}O_{39}]^{m-}$), structurally related to the parent Keggin anions by removal of one MO group, are known. Keggin heteropolyanions can be further modified by substituting at least one of the addenda atoms by another metal ion, M′, giving complexes of the general formula $[XM_{11}M'(H_2O)O_{39}]^{p-}$, which present additional properties [1,2].

Polyoxometalates have gained particular attention due to their applications in many fields such as materials science [3–5], analytical chemistry [2], catalysis [6,7] and medicine [8], resulting from their chemical, structural and electronic properties. One of the most important features of Keggin-type POM anions is their ability to accept a large number of electrons, giving rise to mixed-valence species, which makes them very attractive for use in the preparation of modified electrodes and in electrocatalysis [7,9]. The transition metal-substituted anions may have further redox centres, enlarging the possibilities for electrocatalytic applications [10,11]. Thus, the production of devices using polyoxometalates that maintain and enhance their beneficial properties is of great interest.

In recent years, the construction of self-assembled ultrathin films has attracted considerable attention due to their potential applications in molecular and nano-devices. Layer-by-layer (LBL) self-assembly has proved to be a promising method for the fabrication of ultrathin films. It is based on the alternate adsorption on the substrate surface of oppositely charged species from dilute solutions, and film formation is attributed primarily to electrostatic interactions and van der Waals forces [12–15]. Combinations of cationic and anionic polyelectrolytes or of these with smaller ionic species have been reported. Given the large number of materials which can be easily incorporated into multilayer films, layer-by-layer deposition is a rather general approach for the fabrication of complex surface coatings. This method is of great versatility due to the broad processing window and to the many control parameters that can be changed such as concentration, adsorption time, ionic strength, temperature and pH, among others. It also provides thickness control at the nanometre level, can be easily adapted for automated fabrication, is applicable to any substrate shape and also permits co-assembly with different functional components [16,17].

Owing to these advantages, the layer-by-layer approach has been utilized to fabricate POM-containing multilayer films consisting of synthesized or natural polyelectrolytes. For example, thin films based on large polyoxometalates, such as $[H_3Mo_{57}V_6(NO)_6O_{183}(H_2O)_{18}]^{21-}$ [18], $[Mo_{132}O_{372}(CH_3COO)_{30}(H_2O)_{72}]^{42-}$ [19], $[Co_4(H_2O)_2P_4W_{30}O_{112}]^{16-}$, $[Eu(H_2O)P_5W_{30}O_{110}]^{12-}$ and $[Na(H_2O)P_5W_{30}O_{110}]^{14-}$ [16], have been fabricated using poly(ethylenimine) (positively charged) and poly(styrenesulfonate) (negatively charged) as the anchorage layers and poly(allylamine hydrochloride) (positively charged) as the polycation. Keggin-type polyoxometalates were also used for the preparation of ultrathin multilayer films with polyelectrolytes. Early studies have

* Corresponding author. Fax: +351 234 370084.
E-mail address: ana.cavaleiro@ua.pt (A.M.V. Cavaleiro).

0040-6090/$ – see front matter
doi:10.1016/j.tsf.2010.05.065

been reviewed [9]. Several studies used the parent Keggin silicotungstate $[\alpha\text{-}SiW_{12}O_{40}]^{4-}$ as the anion and, for example, polyaniline [20], chitosan [21], or poly(diallyldimethylammonium chloride) [22] as the counter-cation source. Other Keggin-type and related polyoxometalates such as $[Eu(SiW_{11}O_{39})_2]^{13-}$, $[SiMo_{11}VO_{40}]^{5-}$ and $[ZnW_{11}M(H_2O)O_{39}]^{n-}$ (M = Cr, Mn, Fe, Co, Ni, Cu or Zn) were immobilized on a 4-aminobenzoic acid modified glassy carbon electrode through a layer-by-layer assembly with a quaternized poly(4-vinylpyridine) partially complexed with $[Os(bpy)_2Cl]^{1+/2+}$ as the counterion [23–26]. The use of polymeric cations is not necessary for growing films with Keggin anions. For example, the heteropolyacids $H_3PW_{12}O_{40}$, $H_3PMo_{12}O_{40}$ and $H_4SiMo_{12}O_{40}$ have been used with methyl viologen and with the cationic meso-tetra(4N-methylpyridyl porphyrin) [27]. This cation was also used to immobilize the Keggin-type polyoxometalates $[SiW_{12}O_{40}]^{4-}$, $[EuPW_{11}O_{39}]^{4-}$ [28] and $[SiW_{11}Fe^{III}(H_2O)O_{39}]^{5-}$ [29]. There are only a few examples of the use of transition metal monosubstituted Keggin polyoxotungstate anions in films prepared by the layer-by-layer self-assembly method [26,29].

The present work concerns the fabrication of stable multilayer ultrathin films, consisting of *n* bilayers of metal-substituted polyoxometalates, $[PW_{11}Fe^{III}(H_2O)O_{39}]^{4-}$ ($PW_{11}Fe$) and $[SiW_{11}Fe^{III}(H_2O)O_{39}]^{5-}$ ($SiW_{11}Fe$), with poly(ethylenimine) (PEI), prepared by the layer-by-layer self-assembly method. Growth of the multilayer films adsorbed on a quartz slide was monitored by UV–Vis absorption spectroscopy and the surface morphology of the thin films on a glassy carbon electrode was examined by scanning electron microscopy (SEM). The electrochemical behaviour of the immobilized polyanions and electron transfer to $[Fe(CN)_6]^{3-/4-}$ as electrochemical probe was investigated by cyclic voltammetry. Additionally, the possible application of $(PEI/SiW_{11}Fe)_n$ modified electrodes as a sensor for nitrite reduction was tested.

2. Experimental section

2.1. Reagents and solutions

The potassium salts $K_4[PW_{11}Fe^{III}(H_2O)O_{39}]\cdot 6H_2O$ and $K_5[SiW_{11}Fe^{III}(H_2O)O_{39}]\cdot 13H_2O$ were prepared as described in the literature [30,31]. Both compounds were characterized by thermal and elemental analysis, infrared spectroscopy, and powder X-ray diffraction and the results were in agreement with previously published values [30].

Poly(ethylenimine) (MW = 50,000–100,000; 30 wt.% aqueous solution; branched, consisting of tertiary, secondary and primary amino groups in the ratio of 25/50/25, respectively) was purchased from Polysciences Europe GmbH and was used without further treatment. Sodium chloride (Merck), potassium chloride (Merck), acetic acid (Pronalab), sodium acetate (Carlo Erba), potassium ferricyanide (Merck), sodium nitrite (Merck), buffer solution pH 9 (0.05 M H_3BO_3, 0.05 M KCl, 0.022 M NaOH) (Merck) and other reagents were of analytical grade and were used as received.

Electrolyte solutions for voltammetry were prepared using ultra-pure water (resistivity 18.2 MΩ cm at 25 °C, Direct-Q 3 UV system, Millipore). Solutions with pH 4.0, used for electrochemical studies, were prepared by mixing appropriate amounts of the CH_3COOH (0.1 M) and $NaCH_3COO$ (0.1 M) solutions. Potassium ferricyanide solutions (1.0 mM) were prepared by dissolving the appropriate amount of $K_3[Fe(CN)_6]$ in 1 M KCl.

The solutions used for the film preparation were used immediately after their preparation and degassed with pure nitrogen for at least 10 min.

2.2. Instrumentation and methods

UV–Vis absorption spectroscopy of the $PW_{11}Fe$ and $SiW_{11}Fe$ solutions was performed using a quartz cell with a 0.4 cm path length. A set of 7 solutions of each compound (0.001–0.05 mM) in 0.1 M acetate buffer (pH 4.0) was used to determine the isotropic molar absorption coefficient. The UV–Vis absorption spectra of the multilayer films were recorded on quartz slides. A Jasco V-560 UV–visible spectrophotometer was used in all experiments.

Scanning electron microscopy was conducted on an Analytical FE-SEM SU-70 Hitachi, UHR 1.0 nm/15 kV (1.6 nm/1 kV).

Electrochemical experiments were carried out with a computer controlled potentiostat (PGSTAT-12 /GPES software from Autolab/Ecochemie, Netherlands). A conventional three-electrode compartment cell was used. The auxiliary and reference electrodes were platinum wire (7.5 cm, BAS, MW-1032) and Ag/AgCl (sat. KCl) (BAS, MF-2052), respectively. The working electrode was a glassy carbon disc, GCE, (3 mm diameter, BAS, MF-2012), bare or surface-modified with the POM salts. A combined glass electrode (Hanna Instruments HI 1230) connected to an Inolab pH level 1 pH meter was used for the pH measurements.

Elemental analysis, powder X-ray diffraction, thermogravimetric and FTIR studies were performed as indicated previously [11].

2.3. Preparation of self-assembly $(PEI/POM)_n$ films

Prior to coating, the GCE was conditioned by a polishing/cleaning procedure. The GCE was polished with 1.0 μm diamond polishing compound (Metadi II, Buehler) and aluminium oxide of particle size 0.3 μm (Buehler-Masterprep) on a microcloth polishing pad (BAS Bioanalytical Systems Inc), then the electrode was rinsed with ultra-pure water and finally sonicated, for 5 min in an ultrasonic bath (Branson 2510). The quartz slides were cleaned by placing them in a H_2SO_4/H_2O_2 (3:1) (v/v) hot bath (~80 °C) for 40 min and then in a $H_2O/H_2O_2/NH_3$ (5:1:1) (v/v/v) hot bath (~80 °C) for another 40 min. The cleaned quartz slides were then rinsed with ultra-pure water and dried under a flow of pure nitrogen.

After the cleaning step, the GCE (or quartz slide) was immersed in a 5 mg/mL (0.12 M) PEI solution (in pH = 9.0 buffer) for 20 min. In the aqueous solution of pH = 9, at least 3% of the amino group in PEI is protonated, so that PEI acts as a polycation. The GCE was then immersed in a 0.3 mM POM solution (in pH = 4.0 acetate buffer) for 20 min. Water rinsing and nitrogen drying steps were performed after each immersion. This process was repeated until the desired number of bilayers of PEI/POM was obtained. Studies of multilayer film formation using a 5 mg/mL PEI solution at pH 4.0 were also performed. Additionally, the influence of different deposition times was tested. All measurements were made at room temperature (~20 °C).

3. Results and discussion

Thin multilayer films of iron-substituted Keggin polyoxometalates ($PW_{11}Fe$ or $SiW_{11}Fe$) and protonated poly(ethylenimine) prepared by layer-by-layer self-assembly were deposited on glassy carbon electrodes or on quartz slides, by alternate immersion in aqueous solutions of PEI and of the chosen polyoxoanion. The formation of the multilayer structure via alternate adsorption of cationic PEI and anionic POM on a substrate is represented in Scheme 1. The influence of pH, concentration and time of immersion were studied, in order to find the better deposition conditions. The functionalized electrodes were tested for the electrocatalytic reduction of nitrite.

3.1. Characterization of multilayer $(PEI/POM)_n$ films deposited on quartz slides

UV–Vis spectroscopy was used after the deposition of each bilayer to monitor the growth process of the multilayer films. Fig. 1 shows the UV–Vis spectra of $(PEI/PW_{11}Fe)_n$ and $(PEI/SiW_{11}Fe)_n$ assembled on a quartz slide. The spectra are all similar, presenting three absorption bands; the band positions and shape did not change during multilayer construction. PEI does not absorb above 200 nm, and the films exhibit the characteristic bands of $PW_{11}Fe$ and $SiW_{11}Fe$ near 195, 260 and

340 nm [30]. These bands correspond to charge transfer transitions from the terminal oxygen atoms to tungsten atoms ($O_d \rightarrow W$), across bridge bonds W–O–W ($O_b \rightarrow W$ or $O_c \rightarrow W$) and from oxygen to iron ($O \rightarrow Fe$), respectively. The absorption bands at 260 nm ($PW_{11}Fe$) and 258 nm ($SiW_{11}Fe$) were chosen to monitor film growth. The insets in Fig. 1 show that the absorbance increases almost linearly with the number of deposited layers, suggesting that the quantity of polyoxometalate deposited per bilayer was approximately the same up to seven bilayers for $PW_{11}Fe$ and up to eight for $SiW_{11}Fe$. The inset in Fig. 1(b) also shows the absorbance of $(PEI/SiW_{11}Fe)_n$ multilayers at 258 nm as a function of n for three different deposition times. It can be seen that there is considerable difference between deposition time of 5, 10 or 20 min. Typically, in the literature, an adsorption time between 5 and 20 min for each polyion is used although, in most cases, the major amount of polyelectrolyte was in fact adsorbed within a few minutes [13,14,32,33]. Longer deposition times (30 and 60 min) were also evaluated, besides the ones referred to above. However, saturation was achieved after 20 min since the absorbance values at 200 nm did not increase further for longer deposition times. Cyclic voltammetry tests were in agreement with this, so, except when indicated, 20 min was the time used in the experiments described below.

The surface coverage per layer, Γ, can be estimated from the spectra of the multilayers, according to the Beer–Lambert law

$$\Gamma = A_\lambda / 2m\varepsilon_\lambda \quad (1)$$

where A_λ is the absorbance at the specified wavelength, m is the number of layers and ε_λ is the isotropic molar absorption coefficient ($M^{-1}\,cm^{-1}$) [17]. In aqueous solution (acetate buffer, pH 4) the isotropic molar absorption coefficients for $PW_{11}Fe$ and for $SiW_{11}Fe$ are $\varepsilon_{260} = 9.87\times10^4\,M^{-1}\,cm^{-1}$ and $\varepsilon_{258} = 8.84\times10^4\,M^{-1}\,cm^{-1}$, respectively. Using Eq. (1), this leads to values of the surface coverage of 2.72×10^{-10} mol cm^{-2} for $PW_{11}Fe$ and 3.04×10^{-10} mol cm^{-2} for $SiW_{11}Fe$ for a 20 min deposition time. In the case of $SiW_{11}Fe$, surface coverages of 2.15×10^{-10} mol cm^{-2} and 1.75×10^{-10} mol cm^{-2} were obtained for deposition times of 10 and 5 min. These values are somewhat higher than the 1.00×10^{-10} mol cm^{-2} obtained for $(PMo_{12}/PDDA)_n$ by Wang et al. [34] which they attributed to monolayer coverage. A possible explanation for the values obtained being higher than expected may be the existence of diffuse scattering due to the heterogeneity of the surface. It is known that when a beam is passed through a thin layer of matter its intensity is generally diminished as a consequence of both absorption and scattering. These scattering losses would give rise to a lower intensity of the transmitted beam and thence higher calculated absorbance values and surface coverages.

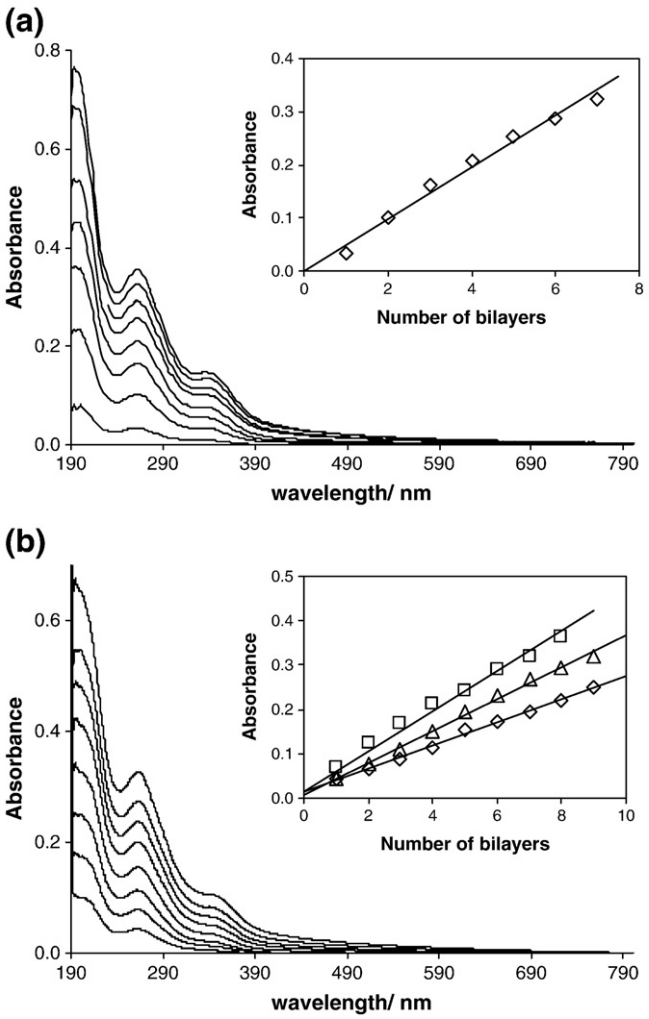

Fig. 1. UV–Vis absorption spectra of (a) $(PEI/PW_{11}Fe)_n$ and (b) $(PEI/SiW_{11}Fe)_n$ multilayers for $n = 0-8$ adsorbed on a quartz slide. The insets in (a) and (b) show the absorbance at (a) 260 nm and (b) 258 nm, as a function of n. The inset in (b) also shows the absorbance as a function of n for different deposition times: (□) 20, (Δ) 10 and (◊) 5 min.

3.2. Scanning electron microscopy characterization

SEM images provide information about the surface morphology and homogeneity of the PEI layer and $(PEI/POM)_n$ multilayer films. Fig. 2 shows SEM images of the PEI layer on a glassy carbon electrode at two magnifications. In Fig. 2(a) it can be seen that after PEI adsorption the surface is fully covered with small white bead-shaped domains of different sizes. Amplification of the image reveals that the darker parts are also covered with PEI (Fig. 2(b)).

Fig. 3 shows representative images upon adsorption of two bilayers of $(PEI/PW_{11}Fe)$ and $(PEI/SiW_{11}Fe)$ at different magnifications. In both cases, a completely-covered surface is observed but the deposited film presents a considerable number of cracks (Fig. 3(a) and (c)). These may be due to the vacuum system used in the SEM equipment and also to the high-energy beam; in fact, it was possible to see the formation of cracks in places where they did not exist previously on increasing the

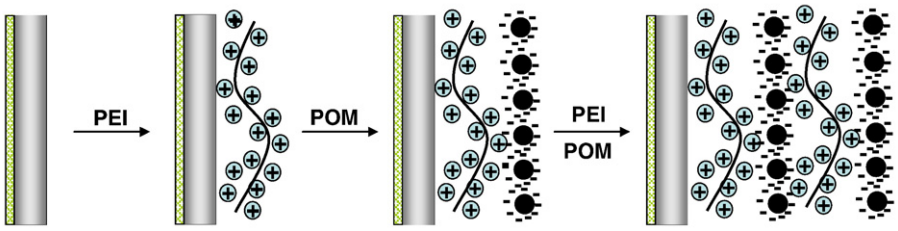

Scheme 1. Schematic diagram of the formation of the multilayer structure via alternate adsorption of cationic PEI and anionic POM on a substrate.

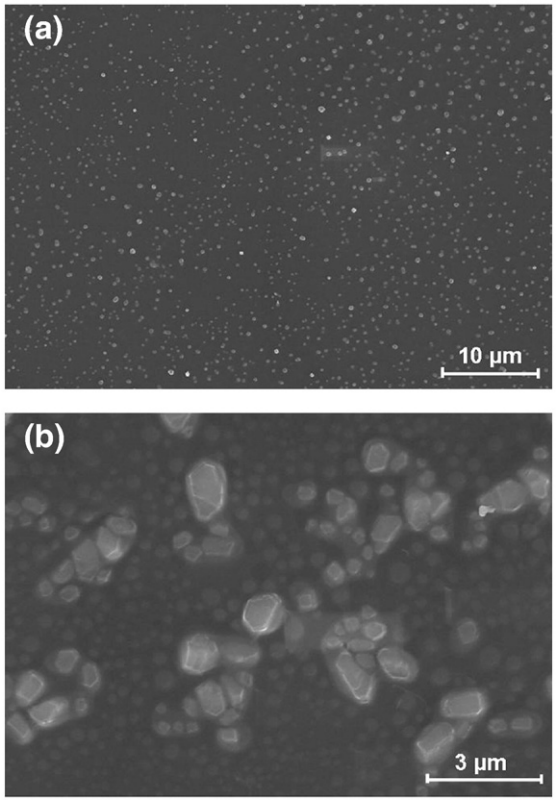

Fig. 2. Typical SEM micrographs for a PEI layer adsorbed on a glassy carbon electrode at different magnifications (a) x2000 and (b) x8000.

magnification. Higher magnification (Figs. 3(b) and 4(d)) reveals the presence of a high density of irregular shaped domains of small micrometric dimensions underneath these cracks.

3.3. Voltammetric behaviour of multilayer films

All voltammetric results presented below were obtained using a concentration of 0.3 mM of POM for film preparation. Studies with electrodes obtained using 1 mM solutions for the same deposition time did not show significant changes in the peak currents. This suggests that, in this concentration range, the concentration of POM has little effect on the amount of POM adsorbed in each layer and, in fact, that the determinant factor for higher adsorption of POM is the amount of available PEI rather than the POM concentration.

In order to ensure reproducible results and as mentioned in Section 2.3 on film preparation, after each immersion the electrode was rinsed with ultra-pure water and dried under a flow of nitrogen. Rinsing removes weakly attached, physically adsorbed molecules, preparing the surface for the next adsorbed layer [33] and guarantees precise increments in the thickness of the layer-by-layer self-assembled films.

To understand the electrochemical behaviour of $(PEI/POM)_n$ films, comparison with the redox behaviour of the POMs in aqueous solution is important. The majority of the voltammetric studies reported for transition metal-substituted Keggin-type anions in aqueous solution have been performed in acidic media [1,10,35,36]. In these conditions, both anions studied in this work presented two consecutive reversible or quasi-reversible 2-electron waves at negative potentials, corresponding to the reduction of W^{VI} atoms [10,35] and another wave at a less negative potential due to the redox process of $Fe^{III/II}$. Both $SiW_{11}Fe$ and $PW_{11}Fe$, studied in different acidic aqueous solutions, presented E_{pa} and E_{pc} values independent of scan rate, suggesting that the electrode reactions are reversible; peak currents were proportional

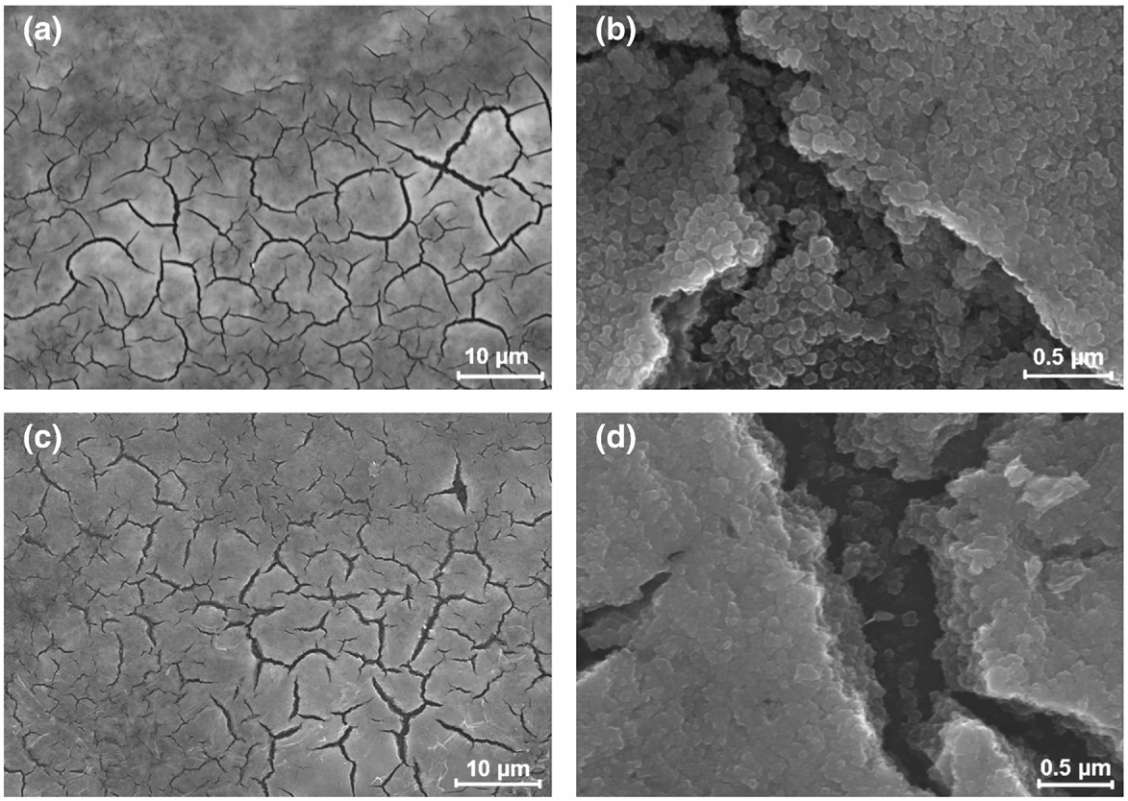

Fig. 3. Representative SEM micrographs of $(PEI/PW_{11}Fe)_2$ and $(PEI/SiW_{11}Fe)_2$ films on a glassy carbon electrode at different magnifications: (a) $(PEI/PW_{11}Fe)_2$ (×1800); (b) $(PEI/PW_{11}Fe)_2$ (×35,000); (c) $(PEI/SiW_{11}Fe)_2$ (×1800) and (d) $(PEI/SiW_{11}Fe)_2$ (×30,000).

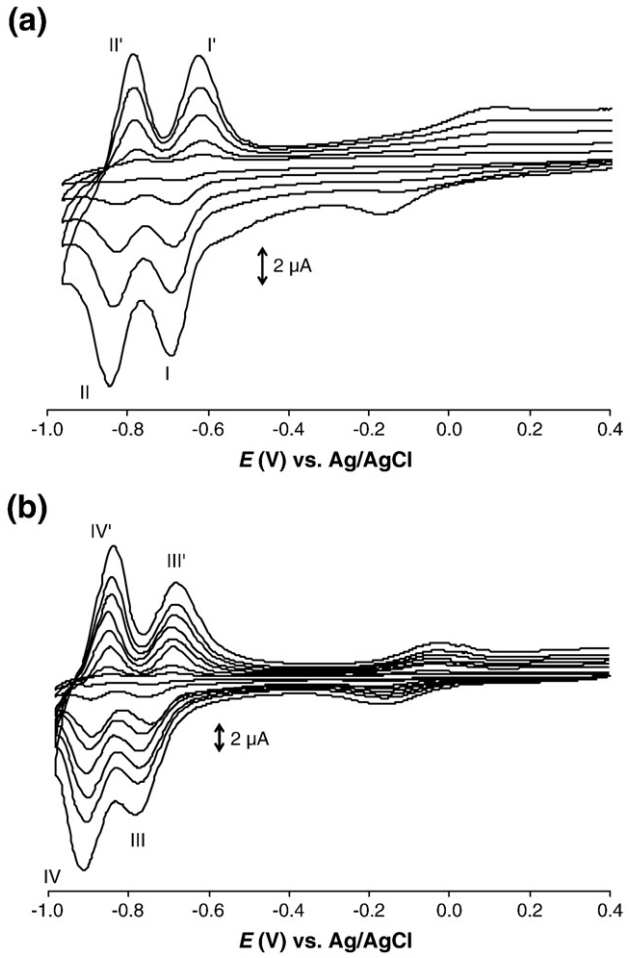

Fig. 4. Cyclic voltammograms for (PEI/POM) bilayer films in $CH_3COOH/NaCH_3COO$ buffer solution (pH 4.0) at different scan rates: (a) 10, 25, 50, 75 and 100 mV s^{-1} for $(PEI/PW_{11}Fe)$ and (b) 10, 25, 50, 75, 100, 125, 150 and 200 mV s^{-1} for $(PEI/SiW_{11}Fe)$.

to the square root of scan rate, indicating that the redox processes were controlled by diffusion [10,35].

Fig. 4 shows cyclic voltammograms for single $(PEI/PW_{11}Fe)$ and $(PEI/SiW_{11}Fe)$ bilayers at different scan rates at pH 4.0, which demonstrate that the electrochemical properties of the two POMs studied are maintained in the multilayer films. Since PEI is not electroactive, its presence is not reflected in the cyclic voltammograms. Under the conditions used, two quasi-reversible two-electron waves (I–I′, II–II′ for $PW_{11}Fe$, III–III′ and IV–IV′ for $SiW_{11}Fe$) were observed, with reduction peaks at −680 and −838 mV for $PW_{11}Fe$ and at −750 and −905 mV for $SiW_{11}Fe$ vs. Ag/AgCl, corresponding to the reduction of tungsten atoms. A pair of peaks for the one-electron reduction/oxidation of $Fe^{III/II}$ is also observed in both cases. In the experimental timescale employed (scan rates in the range 10 to 100 mV s^{-1} for $(PEI/PW_{11}Fe)$ and 10 to 200 mV s^{-1} for $(PEI/SiW_{11}Fe)$) the values of peak potential changed only slightly with scan rate, and the ratio of anodic to cathodic peak currents was close to 1.

It was found that the cathodic and anodic peak currents of the first W wave were directly proportional to the scan rate, which indicates a surface-confined process. This is consistent with the early finding of S. Liu et al. for $[Co_4(H_2O)_2P_4W_{30}O_{112}]^{16-}$, $[Eu(H_2O)P_5W_{30}O_{110}]^{12-}$ and $[Na(H_2O)P_5W_{30}O_{110}]^{14-}$ [16], and of B. Xu et al. for $K_6[P_2W_{18}O_{62}]\cdot 14H_2O$ [37]. The number of electrons transferred in the tungsten redox processes is obtained by comparison of the peak currents for the $Fe^{III/II}$ couple with those of the first tungsten reduction process and indicate a 2-electron process (i.e. two coincident one-electron $W^{VI/V}$ reductions). Note that the peak currents for the $Fe^{III/II}$ couple are influenced by slower kinetics of this process (the peak-to-peak separation is substantially higher than for the first W wave), thus the I_p for the $Fe^{III/II}$ reduction is certainly less than for a fully reversible process. In addition, the anodic/cathodic peak-to-peak separation (ΔE_p) for the tungsten waves was ca. 50–60 mV instead of zero, which would have been expected for a reversible surface process.

Comparison of the electrochemical behaviour of the multilayer $(PEI/SiW_{11}Fe)_n$ film with that of the potassium salt of $SiW_{11}Fe$ in pH 4.0 aqueous solution [10] shows that there are no significant differences in the peak potentials, but the peaks are broader than in solution. This broadening may be related to the large coulombic repulsion between the negative sites of highly-charged polyanions in the same layer, as in [38]. It also demonstrates that the PEI layers do not block electron transfers between the immobilized anions of $SiW_{11}Fe$.

Cyclic voltammograms for $(PEI/PW_{11}Fe)_n$ and $(PEI/SiW_{11}Fe)_n$ multilayer films with different numbers of layers are presented in Fig. 5. In both cases, the cathodic peak potentials shift to more negative values by approximately 10 to 20 mV and the anodic peak potentials for $PW_{11}Fe$ shift to more positive values with an increase in the number of layers. Plots of peak current vs. the number of bilayers (n), show linear growth up to $n=5$ for $PW_{11}Fe$ and $n=6$ for $SiW_{11}Fe$. Above these numbers of bilayers, peak currents begin to show a negative deviation from linearity, which can be ascribed to effects of film resistance, i.e.

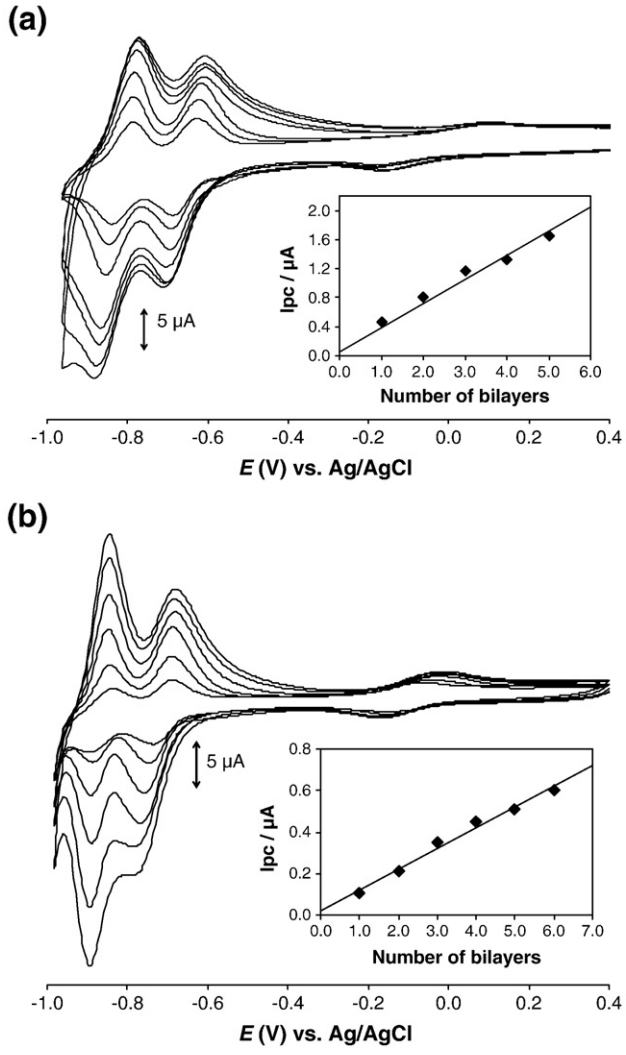

Fig. 5. Cyclic voltammograms for (a) $(PEI/PW_{11}Fe)_n$ and (b) $(PEI/SiW11Fe)_n$ multilayer films in $CH_3COOH/NaCH_3COO$ buffer solution (pH 4.0) for $n=7$ for $PEI/PW_{11}Fe$ and 6 for $PEI/SiW_{11}Fe$, $v=100$ mV s^{-1}. The insets show the peak currents vs. the number of bilayers.

difficulty of transferring electrons through the film to the electrode substrate.

In order to gain more insight into the prerequisites for the good deposition of multilayer films, the influence of two polycation solutions with different pH values on the growth characteristics of PEI/$SiW_{11}Fe$ multilayers was studied. Different adsorption times of the polycation PEI and polyanion $SiW_{11}Fe$ were also tested.

The effect of pH on the layer-by-layer self-assembly method is evident, but complex [17]. Apart from any changes in ionic strength of the buffer solutions used, a change in pH may modify the charge density of polyelectrolytes due to protonation–deprotonation equilibria: an increased charge density of the adsorbing polymer will favour thinner adsorption layers, whereas increasing charge density at the surface will favour thicker adsorbed layers [39]. Therefore, the effect of pH on layer-by-layer film growth is not clear *a priori*. To study the pH effect, two 5 mg/mL PEI solutions were used in LbL film preparation, one in a pH 9.0 and the other in a pH 4.0 buffer solution. No differences in the peak potentials were observed and peak currents increased linearly with the number of layers in both cases. However, the peak currents were lower when using the modified electrodes prepared with the PEI solution at pH 4.0 than at pH 9.0, although the peaks obtained were better resolved.

The influence of deposition time on the growth of multilayer films on the carbon electrodes was tested using different immersion times per anionic or polycationic layer (60, 30, 20, 15 and 10 min). Since saturation was achieved using 20 min deposition time, only 20, 15 and 10 min will be discussed here. For these three adsorption times used, there was no difference in the peak currents up to the (PEI/$SiW_{11}Fe$)$_4$ multilayer but differences became apparent for (PEI/$SiW_{11}Fe$)$_5$ and subsequent multilayers. An adsorption time of 20 min results in the largest amount of adsorbed material (higher peak currents). For 10 and 15 min adsorption times, after the (PEI/$SiW_{11}Fe$)$_6$ multilayer peak current saturation is obtained. Several studies indicate that polyelectrolyte adsorption is a two-step process where most polymer chains are anchored during a fast initial step and then the growth of the film slows down until the surface charge becomes completely inverted [13,14,32,40]. This second step may take much longer. Taking this into account, it is probable that 10 and 15 min are not sufficient to achieve total charge reversal with respect to the previous layer, thus leading a smaller adsorption of the next layer and consequent lower peak currents.

Surface coverage can be calculated from cyclic voltammetry according to the equation

$$\Gamma = \left(4I_{pa}RT\right) / \left(n^2F^2\nu A\right) \quad (2)$$

where I_{pa} is the anodic peak current (amperes), n is the number of electrons transferred (2 in this case), ν is the scan rate (V s^{-1}), A is the geometric area of the electrode (0.0725 cm^2), R is the gas constant (8.314 J K^{-1} mol^{-1}), T is the temperature (298 K) and F is Faraday's constant (96,485 °C mol^{-1}) [38]. In order to obtain the surface coverage, peak currents were plotted against scan rate (10 to 100 mV s^{-1}) and the value of I_{pa}/ν obtained was used to calculate surface coverage using Eq. (2). This led to a surface coverage of 1.29×10^{-10} mol cm^{-2} for $PW_{11}Fe$ and 1.09×10^{-10} mol cm^{-2} for $SiW_{11}Fe$.

Assuming a close geometric packing of POM clusters and the data from scanning tunnelling microscopy observation of Keggin clusters deposited on a gold surface [41] to estimate monolayer coverage, Wang et al. [34] calculated a value of 1.25×10^{-10} mol cm^{-2}. Comparing this with our values of surface coverage obtained by cyclic voltammetry, ours correspond to monolayer coverage. Nevertheless, the surface coverages estimated by UV–visible spectroscopy are somewhat higher (2.72×10^{-10} mol cm^{-2} for $PW_{11}Fe$ and 3.04×10^{-10} mol cm^{-2} for $SiW_{11}Fe$), but are calculated ignoring the possibility of scattering and assuming that the molar absorption coefficients of the Fe-polyoxometalates are the same in solution and in the films, which is not certain. The surface coverages reported in the literature calculated by cyclic voltammetry are usually lower than those obtained from UV–visible spectroscopy [16,17].

3.4. Permeability of multilayer films

Electrochemistry can be employed to assess film permeability and as a sensitive probe of structural changes in the (PEI/POM)$_n$ films. In particular, the passivating abilities of different films can be compared using cyclic voltammetry via peak currents and voltammogram shapes. Many groups have used the $[Fe(CN)_6]^{3-/4-}$ redox couple to study the permeability of multilayer films [16,42–45]; however, studies of electron transfer at films containing polyoxometalates are few. Liu et al. showed that the permeability towards these species can be tailored through the multilayer construction and deposition conditions [16]. Also, Gao et al. investigated how the number of layers in the multilayer films influences the shape of the cyclic voltammograms [45].

Cyclic voltammograms of $[Fe(CN)_6]^{3-/4-}$ were recorded to investigate how they changed with the number of bilayers of (PEI/$PW_{11}Fe$) and the influence of the nature of the final layer. A more reversible voltammogram indicates better access to the electrode substrate, which should result in higher peak currents. Fig. 6(a) shows cyclic voltammograms of $[Fe(CN)_6]^{3-/4-}$ at the electrode modified with (PEI/$PW_{11}Fe$)$_n$ for $n=1, 2, 4$ and 6. These results show that for an electrode coated with a single (PEI/$PW_{11}Fe$) bilayer (Fig. 6(a1)) the cyclic voltammogram exhibits quasi-reversible properties, indicating that the probe diffuses freely through the layer and undergoes electron transfer at the electrode surface. Increasing the number of multilayers from one to four leads to a

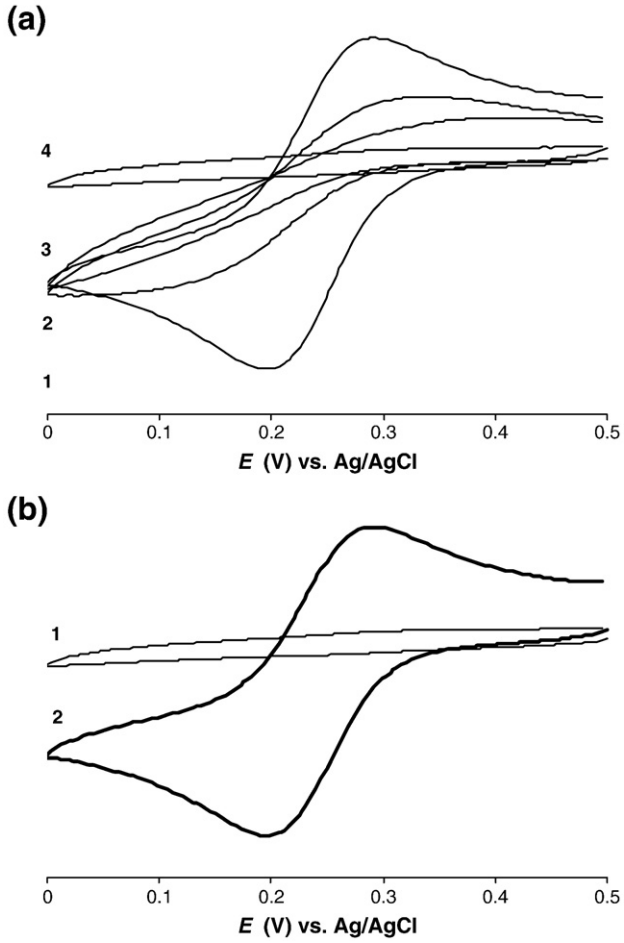

Fig. 6. Cyclic voltammograms of $[Fe(CN)_6]^{3-/4-}$ (1 mM, 1 M KCl) $\nu=100$ mV s^{-1}, at modified electrodes with (a) (PEI/$PW_{11}Fe$)$_n$ for (1) $n=1$; (2) 2; (3) 4 and (4) 6; (b) 1 — (PEI/$PW_{11}Fe$)$_6$ and 2 — (PEI/$PW_{11}Fe$)$_6$/PEI.

decrease in peak currents and peak broadening (Fig. 6(a1–3)). A further increase of n until 6 leads to an electrode with plateau-shaped current characteristics (Fig. 6(a4)). These observations show that an increased number of multilayers with a terminal negatively charged $PW_{11}Fe$ anion leads to a decrease in the number of hexacyanoferrate ions which reach the electrode substrate. This is attributable to electrostatic repulsion of $[Fe(CN)_6]^{3-/4-}$ by the negatively charged $PW_{11}Fe$ anion; similar results were obtained for $[Co_4(H_2O)_2(PW_9O_{34})_2]^{10-}$ clusters [45], compounded by the greater distance the ions need to diffuse through the film, as well as fewer pathways, as it becomes thicker.

When the outermost layer is the positively charged PEI, deposited on $(PEI/PW_{11}Fe)_6$, the quasi-reversible properties in the cyclic voltammogram of $[Fe(CN)_6]^{3-/4-}$ are restored (Fig. 6(b)). This indicates that whenever the layered film is terminated with the positively charged PEI layer, there ceases to be any barrier to transport through the film because of the electrostatic attraction of $[Fe(CN)_6]^{3-/4-}$ from the terminal positively charged PEI layer. The voltammogram is similar to that of a bare electrode, independent of film thickness.

The stability and reproducibility of these LbL-modified electrodes were also tested. For five electrode assemblies prepared under identical conditions the relative standard deviation of the peak current for the first tungsten reduction wave was 14.9% for $(PEI/PW_{11}Fe)_n$ and 4.3% for $(PEI/SiW_{11}Fe)_n$, which can be explained through the known stability of the respective POM anions [10]. Peak potentials did not change. Modified electrodes were kept for 1, 3 or 5 days in the air to examine stability, and there was no change in the shape and height of the redox waves.

3.5. Electrocatalytic properties of $(PEI/SiW_{11}Fe)n$ multilayer films

The applicability of POM species, as a reduction electrocatalyst, is based on the fact that the reduced form, which is the catalytic mediator, can provide a large number of electrons at a suitable, not too negative, potential. Heteropolyanions, in general, have been proved to be excellent catalysts for the electroreduction of various species [46–48] and have been extensively exploited. For example, our group observed that tetrabutylammonium-$SiW_{11}Fe$ modified electrodes can reduce nitrite [10], Dong et al. observed that the parent $[SiW_{12}O_{40}]^{4-}$ could be used as electrocatalyst for the reduction of nitrite [49] and Toth and Anson applied the iron-substituted Keggin-type POMs, $[XW_{11}Fe^{(III)}(H_2O)O_{39}]^{n-}$, where X = P, As, Si or Ge as catalysts for the reduction of hydrogen peroxide and nitrite [36,46].

Nitrite was chosen to test the electrocatalytic properties of the $(PEI/SiW_{11}Fe)n$ multilayer films. In acidic solutions, nitrite is protonated to HNO_2 and can disproportionate, although the rate of this process is known to be low. It is normally assumed that nitrous acid is the reactive form of nitrite between pH 2 and 8 in the case of the electrocatalysis with iron-substituted polyoxotungstates [46].

Fig. 7 presents cyclic voltammograms for the $(PEI/SiW_{11}Fe)_7$ multilayer film modified electrode in the absence and in the presence of increasing concentrations of nitrite in the interval from 0 to 0.7 mM, at a scan rate 10 mV s^{-1}. The inset of Fig. 7 shows the catalytic peak current at −0.77 V vs. the concentration of nitrite up to 0.7 mM.

As is known, the electroreduction of nitrite requires a large overpotential, and no response is observed in the range of potentials used at the bare electrode in a solution containing NO_2^-. At pH 4.0, the reduction wave associated with the $Fe^{III/II}$ couple is almost unaffected by the addition of NO_2^-, but the two-electron reduction waves of the $SiW_{11}Fe$ anion that appear at more negative potentials are significantly enhanced by the addition of nitrite. A linear range for the catalytic current can be defined for a nitrite concentration up to 0.7 mM, as shown in the inset.

Although the $Fe^{III/II}$ couple is almost unaffected by the addition of nitrite, the presence of the iron centre is essential for the catalysis because nitrite has no effect on the cyclic voltammograms of the lacunary derivative $KSiW_{11}$ [10], despite the fact that this anion exhibits a voltammetric response at potentials similar to those of $KSiW_{11}Fe$ anions.

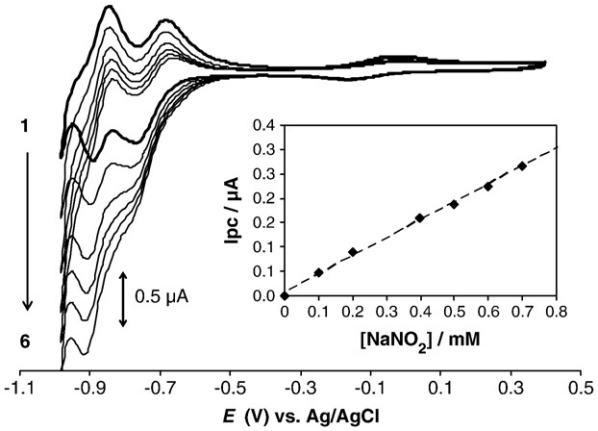

Fig. 7. Cyclic voltammograms of GCE/$(PEI/SiW_{11}Fe)_7$ in pH 4.0 buffer solution at a scan rate of 10 mV s^{-1} obtained in the absence and in the presence of added concentrations of nitrite: 1) 0; 2) 0.2; 3) 0.4; 4) 0.5; 5) 0.6 and 6) 0.7 mM. The inset shows the catalytic peak current at −0.77 V vs. the concentration of nitrite.

4. Conclusions

The present work has demonstrated that $(PEI/PW_{11}Fe)_n$ and $(PEI/SiW_{11}Fe)_n$ multilayer films can be prepared on glassy carbon electrodes using layer-by-layer self-assembly and that the electrochemical properties of the two POMs are maintained. The effect of scan rate in cyclic voltammetry leads to the conclusion that the first tungsten reduction process for $PW_{11}Fe$ and $SiW_{11}Fe$ is a surface-confined process. UV–Vis spectroscopy demonstrated that the amount of POM adsorbed per deposition step is almost constant.

Use of $[Fe(CN)_6]^{3-/4-}$ electrochemical probe showed that terminal negatively charged POMs lead to electrostatic repulsion as well as less penetration through to the electrode surface and that this effect increases with the number of multilayers. When the outermost layer is positively charged, this ceases and the response is the same as that of the bare electrode substrate, independent of film thickness.

The $(PEI/SiW_{11}Fe)_n$ multilayer films also exhibited electrocatalytic activity towards the reduction of nitrite.

Acknowledgments

The authors thank Fundação para a Ciência e a Tecnologia (FCT) for financial support (project POCI 2010-Feder-POCI/QUI/56534/2004). Diana M. Fernandes acknowledges FCT for her PhD grant SFRH/BD/30797/2006. Thanks are also due to CICECO and the University of Aveiro.

References

[1] M.T. Pope, Heteropoly and Isopoly Oxometalates, Springer Verlag, Berlin, 1983.
[2] D.E. Katsoulis, Chem. Rev. 98 (1998) 359.
[3] J.M. Clemente-Juan, E. Coronado, Coord. Chem. Rev. 193 (1999) 361.
[4] P. Gomez-Romero, Adv. Mater. 13 (2001) 163.
[5] E. Coronado, C. Giménez-Saiz, C.J. Gómez-Garcia, Coord. Chem. Rev. 249 (2005) 1776.
[6] C.L. Hill, C.M. Prosser-McCartha, Coord. Chem. Rev. 143 (1995) 407.
[7] B. Keita, L. Nadjo, J. Mol. Catal. A-Chem. 262 (2007) 190.
[8] J.T. Rhule, C.L. Hill, D.A. Judd, Chem. Rev. 98 (1998) 327.
[9] M. Sadakane, E. Steckhan, Chem. Rev. 98 (1998) 219.
[10] D.M. Fernandes, S.M.N. Simões, H.M. Carapuça, A.M.V. Cavaleiro, Electrochim. Acta 53 (2008) 6580.
[11] M.S. Balula, J.A. Gamelas, H.M. Carapuça, A.M.V. Cavaleiro, W. Schlindwein, Eur. J. Inorg. Chem. (2004) 619.
[12] G. Decher, Science 277 (1997) 1232.
[13] S.T. Dubas, J.B. Schlenoff, Macromolecules 32 (1999) 8153.
[14] P. Bertrand, A. Jonas, A. Laschewsky, R. Legras, Macromol. Rapid Commun. 21 (2000) 319.

[15] F.N. Crespilho, V. Zucolotto, O.N. Oliveira Jr, F.C. Nart, Int. J. Electrochem. Sci. 1 (2006) 194.
[16] S. Liu, D.G. Kurth, B. Bredenkotter, D. Volkmer, J. Am. Chem. Soc. 124 (2002) 12279.
[17] G. Decher, J.B. Schlenoff, Multilayer Thin Films, Wiley – VCH, 2003.
[18] F. Caruso, D.G. Kurth, D. Volkmer, M.J. Koop, A. Müller, Langmuir 14 (1998) 3462.
[19] D.G. Kurth, D. Volkmer, M. Ruttorf, B. Richter, A. Müller, Chem. Mater. 12 (2000) 2829.
[20] Y. Wang, C. Guo, Y. Chen, C. Hu, W. Yu, J. Colloid Interface Sci. 264 (2003) 176.
[21] Y. Feng, Z. Han, J. Peng, J. Lu, B. Xue, L. Li, H. Ma, E. Wang, Mater. Lett. 60 (2006) 1588.
[22] S. Li, E. Wang, C. Tian, B. Mao, Y. Song, C. Wang, L. Xu, Mater. Res. Bull. 43 (2008) 2880.
[23] L. Cheng, J. Liu, S. Dong, Anal. Chim. Acta 417 (2000) 133.
[24] S. Zhai, Y. Chen, S. Wang, J. Jiang, Talanta 63 (2004) 927.
[25] L. Cheng, S. Dong, J. Electroanal. Chem. 481 (2000) 168.
[26] J. Liu, L. Cheng, S. Dong, Electroanalysis 14 (2002) 569.
[27] D. Martel, M. Gross, J. Solid State Electrochem. 11 (2007) 421.
[28] G. Bazzan, W. Smith, L.C. Francesconi, C.M. Drain, Langmuir 24 (2008) 3244.
[29] K. Shiu, F.C. Anson, J. Electroanal. Chem. 309 (1991) 115.
[30] F. Zonnevijlle, C.M. Tourne, G.F. Tourne, Inorg. Chem. 21 (1982) 2751.
[31] C.M. Tourne, G.F. Tourne, S.A. Malik, T.J.R. Weakly, J. Inorg. Nucl. Chem. 32 (1970) 3875.
[32] D.G. Kurth, R. Osterhout, Langmuir 15 (1999) 4842.
[33] Y. Lvov, K. Ariga, M. Onda, I. Ichinose, T. Kunitake, Colloid Surf. A-Physicochem. Eng. Asp. 146 (1999) 337.
[34] B. Wang, R.N. Vyas, S. Shaik, Langmuir 23 (2007) 11120.
[35] F.A.R.S. Couto, A.M.V. Cavaleiro, J.D. Pedrosa de Jesus, J.E.J. Simão, Inorg. Chim. Acta 281 (1998) 225.
[36] J.E. Toth, F.C. Anson, J. Electroanal. Chem. 256 (1988) 361.
[37] B. Xu, L. Xu, G. Gao, W. Guo, S. Liu, J. Colloid Interface Sci. 330 (2009) 408.
[38] L. Cheng, J.A. Cox, Electrochem. Commun. 3 (2001) 285.
[39] D. Yoo, S. Shiratori, M. Rubner, Macromolecules 31 (1998) 4309.
[40] F. Hua, Y.M. Lvov, The New Frontiers of Organic and Composite Nanotechnology, 2008, p. 1.
[41] W.G. Klemperer, C.G. Wall, Chem. Rev. 98 (1998) 297.
[42] J.J. Harris, M.L. Bruening, Langmuir 16 (2000) 2006.
[43] V. Pardo-Yissar, E. Katz, O. Lioubashevski, I. Willner, Langmuir 17 (2001) 1110.
[44] J. Dai, A.W. Jensen, D.K. Mohanty, J. Erndt, M.L. Bruening, Langmuir 17 (2001) 931.
[45] S. Gao, T. Li, X. Li, R. Cao, Mater. Lett. 60 (2006) 3622.
[46] J.E. Toth, F.C. Anson, J. Am. Chem. Soc. 111 (1989) 2444.
[47] T. McCormac, B. Fabre, G. Bidan, J. Electroanal. Chem. 427 (1997) 155.
[48] L. Wang, D. Xiao, E. Wang, L. Xu, J. Colloid Interface Sci. 285 (2005) 435.
[49] S. Dong, X. Xi, M. Tian, J. Electroanal. Chem. 385 (1995) 227.